Composition, Tensile Properties, and Dispersion of Polypropylene Composites Reinforced with Viscose Fibers

T. Paunikallio, M. Suvanto, T. T. Pakkanen

Department of Chemistry, University of Joensuu, P.O. Box 111, FIN-80101 Joensuu, Finland

Received 7 April 2003; accepted 21 July 2003

ABSTRACT: The reinforcement mechanics of viscose-fiber-reinforced polypropylene (PP) composites were studied. The effect of the coupling agent, maleated polypropylene (MAPP), was of special interest. The fibers, coupling agent, and PP were extruded and injection-molded. The composition, mechanical properties, fracture morphology, and dispersion of the composites were examined. Thermogravimetric analysis showed that the fiber content in the tensile specimens varied slightly with the sample location; however, the differences in the values were within 1.0%. Scanning electron microscopy images of the fracture surfaces of the composites showed that the surfaces of the composites without MAPP were covered with fibers pulled out from the matrix. A lack of adhesion further appeared as a cracked matrix–fiber interface. A new scanning thermal microscopy method, microthermal analysis, was used to study the dispersion of the fibers in the composites. Local thermal analyses gave further information about the location of the fibers. © 2003 Wiley Periodicals, Inc. J Appl Polym Sci 91: 2676–2684, 2004

Key words: composites; reinforcement; mechanical properties

INTRODUCTION

Plastic composites that are filled or, if the interfacial adhesion is good, reinforced with wood or natural materials, especially wood fibers, are becoming attractive alternatives to glass–plastic composites.[1] Some natural fiber composites, such as composites reinforced with flax fibers, possess mechanical properties similar to those of glass–plastic composites; however, the price of flax fiber is higher than that of glass fiber.[1] Some properties of natural fibers are better than those of glass or carbon fibers. These include low density, high toughness, reduced respiratory irritation and machine abrasion, and biodegradability.[2] The main problems with wood–plastic composites are variations in the quality and structure of the fiber, poor compatibility between the matrix and fiber, limited thermal stability, and swelling of the fiber.[3]

Various chemical methods have been developed to improve the mechanical properties of wood–plastic composites. One of the most promising is the use of compatibilizers and coupling agents to improve the adhesion between the matrix and fiber. Over 40 different coupling agents have been used in wood–plastic composites,[4] silanes and maleated polypropylenes (MAPPs) being the most common.

Correspondence to: T. T. Pakkanen (tuula.pakkanen@joensuu.fi).

Journal of Applied Polymer Science, Vol. 91, 2676–2684 (2004)

Microscopy methods such as scanning electron microscopy (SEM) and optical microscopy have been used to obtain information about the dispersion and morphology of composites. Recently, atomic force microscopy (AFM) has been applied to composites, along with SEM and optical microscopy. AFM has been used for glass and carbon-fiber composites to obtain information about the fiber dispersion and the fiber–matrix interphase.[5–7] AFM can also be used to characterize wood-fiber surfaces.[8,9]

The purpose of this work was to study the reinforcement of polypropylene (PP) with viscose fibers. MAPP was used as a coupling agent. The influence of the coupling agent on the tensile properties was examined, and the mechanism of reinforcement was studied by an examination of the composition of the injection-molded composites by thermogravimetric analysis (TGA); the dispersion was studied with SEM. Also, the suitability of a new AFM method, microthermal analysis (micro-TA), was tested for the study of the dispersion and for the local thermal analysis of the composite surfaces.

EXPERIMENTAL

Materials and pretreatments

The PP was HD120MO (Borealis, Porvoo, Finland), and the MAPP was Polybond 3200 (Crompton Uniroyal Chemical, Middlebury, CT). The manufacturer of the viscose fiber (Br) was Säteri OY (Valkeakoski, Finland). The staple length was 6 mm. The fiber was

TABLE I
TGA Results of the Composite Series A, B, and C

Series	MAPP (wt %)	Fiber content in the extrusion feed (wt %)	Fiber content determined by TGA (wt %)
Composite A	0	40.0	37.0
Composite B	3	39.5	36.9
Composite C	6	39.1	35.7

Seven molded specimens were prepared in each series.

oven-dried at 60°C for 24 h before being handled and was used without further purification. After a liquid-nitrogen treatment, PP and MAPP were ground in an IKA A10 laboratory mill (Ika-Werke GmbH & Co, Staufen, Germany).

Methods

Preparation of the composites

Three series of PP/viscose-fiber composites were prepared, with 40% fiber and (A) 0% MAPP, (B) 3% MAPP, or (C) 6% MAPP (see Table 1). The polymers and the fiber were pre-extruded under a nitrogen gas flow with a DSM twin-screw miniextruder (Geleen, The Netherlands). The composite material was then pelletized, the pellets were extruded, and the extruded mixture was injection-molded. The preparation parameters are shown in Table II. Tensile specimens of pure PP were prepared for a comparison of the tensile properties with those of the composites. The PP specimens were prepared without pre-extrusion. The preparation parameters for the PP specimens were as follows: extrusion time = 5 min, mold temperature = 40°C, and injection pressure = 5 bar. The extrusion temperature (192°C) and the speed of the screws (80 rpm) were the same as those for the PP–fiber composites.

Mechanical testing

Mechanical tests were carried out with material testing equipment from Zwick (Z010/TH2A model 2001; Ulm, Germany). Calculations were performed with TestXpert (version 8.1; Zwick GmbH, Ulm, Germany) software. The crosshead speed was 50 mm/min. A least five standard tensile specimens were tested for each series. The specimens were stored at the ambient temperature (22–23°C) and humidity for 2 days before the testing. The tensile strength, tensile modulus (taken at a strain value of 0.1%), fracture energy, yield strength, and elongation at fracture were measured by standard methods.

SEM

The tensile fracture surfaces of the composites were studied with a Leo 1550 scanning electron microscope operated at 5 kV. The sample surfaces were sputtered with gold before the measurements.

Micro-TA

Micro-TA measurements were made with an Explorer 4400-11 atomic force microscope system with micro-TA facilities (ThermoMicroscopes Inc., Sunnyvale, CA). Images were recorded and local thermal analyses were carried out with TA Instruments (Sunnyvale, CA) μTALab NT V 1.01 and thermal solution programs. The resolution for obtaining images was 200 lines per scan. The heating rate for the local thermal analysis was 10°C/s, and the temperature range was 50–200°C. Temperature calibration was performed with a poly(ethylene terephthalate) sample at the ambient air temperature. The samples were cut with a Leica RM 2165 microtome (Leica Microsystems, Nussloch, Germany) from the center of the tensile specimens after the tensile test. A diamond blade was used in the microtome, and the cutting speed was 1 mm/s.

TGA

Mass-loss/temperature curves were obtained with a Mettler–Toledo DSC821^e device (Greifensee, Switzerland). The fiber, PP, and composite samples were heated from 40 to 600°C. The heating rate was 20°C/min. Nitrogen or synthetic air was used as a purge gas. The gas flow rate was 50 mL/min. The onset temperatures were obtained with a relative method in which the mass lost was 5%. The device was calibrated with indium and aluminum standards. The nitrogen gas flow during calibration was 50 mL/min.

RESULTS AND DISCUSSION

Composition of the composites

Three series of composites (A, B, and C) with MAPP contents of 0–6% (with respect to the fiber weight)

TABLE II
Parameters for Extrusions and Injection Molding

	Extruder temperature (°C)	Time (min)	Screws (rpm)
Pre-extrusion	192	4	80
Extrusion	192	3	80
	Mold temperature (°C)	**Cylinder temperature (°C)**	**Pressure (bar)**
Injection molding	125	190	7

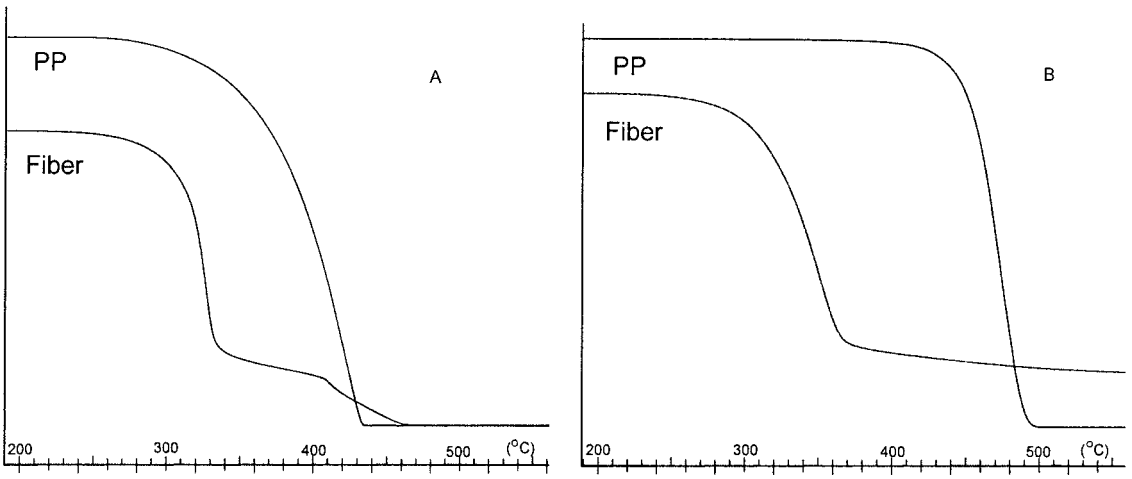

Figure 1 TGA curves of PP and viscose fibers in (A) air and (B) nitrogen purge gases.

were prepared by extrusion and injection molding. The compositions of the injection-molded composites were determined by the study of the thermal degradation of the fiber, PP, and composites by TGA at 40–600°C. First, the thermal degradation of the fiber and the PP matrix was separately studied by TGA with two different purge gases: synthetic air and nitrogen. The TGA curves are shown in Figure 1, and the corresponding numerical values are given in Table III.

A comparison of the shapes of the curves and the onset temperatures (Table III) of the fiber in these two different purge gases clearly reveals the effect of the purge gas on the thermal behavior. The residue is greater and the onset temperature of the fiber is higher when nitrogen is used as a purge gas. When air is the purge gas, a second mass-loss step appears in the thermogram. The shoulder around 400°C and the differences in the TGA data imply that the kinetics and mechanics of the thermal degradation of the fiber are different in the two gases. According to the literature,[10,11] three steps can be distinguished when cellulose is thermally degraded in the presence of air. The first step (300–400°C) generates aliphatic char and volatiles, and the mass lost in this step is about 70%. These results are in agreement with our findings. In the second step (400–600°C), the rest of the char is oxidized, and the rest of the mass consumed. The second mass loss in this study agrees with this and with the much greater amount of residue when nitrogen is used as a purge gas (oxidation is prevented). The third step occurs above 600°C, at temperatures not examined in this study.

TABLE III
TGA Results for Viscose Fibers and PP

Material	Onset temperature in air (°C)	Mass lost in air (%)	Onset temperature in nitrogen (°C)	Mass lost in nitrogen (%)
Viscose fibers	247	95.2	256	78.8
PP	277	99.8	415	99.7

A comparison of the thermal degradation of PP in these two purge gases reveals two distinct differences. First, the onset temperature is 100°C lower in air than in a nitrogen atmosphere (Table III and Fig. 1). Wielage et al.[12] reported similar results for untreated and maleic anhydride grafted PP fibers. Second, the amount of the residue is slightly lower in air than in a nitrogen atmosphere (Table III). However, the residues of PP in both cases are below 0.3 wt %.

TGA curves of the composites were recorded in nitrogen. When air was used as the purge gas, the lower onset temperature of the PP degradation caused the TGA curves of the fiber and PP to overlap. The determination of the fiber composition in the composites was, therefore, difficult in air. The overlap of the TGA curves in the nitrogen atmosphere was minor, and the fiber content of the composites could be determined fairly accurately by the measurement of the mass loss of PP (%) in the temperature region of 400–600°C and by the subtraction of the value from 100%. This method assumes, however, that the degradation of the fiber and PP in the composites is similar to the degradation of the separate materials, that PP alone degrades at 400–600°C, and that the degradation of PP is complete. Figure 2 presents a typical TGA curve of a composite in a nitrogen atmosphere. Earlier, TGA was applied to the determination of the fiber content of plastic composites containing inorganic fibers,[13] but it evidently has not been applied to composites containing organic fibers.

The fiber contents of composites A, B, and C were studied for samples A4, B4, and C4, which were taken from the centers of the tensile specimens. The results are given in Table I. No notable correlation is indi-

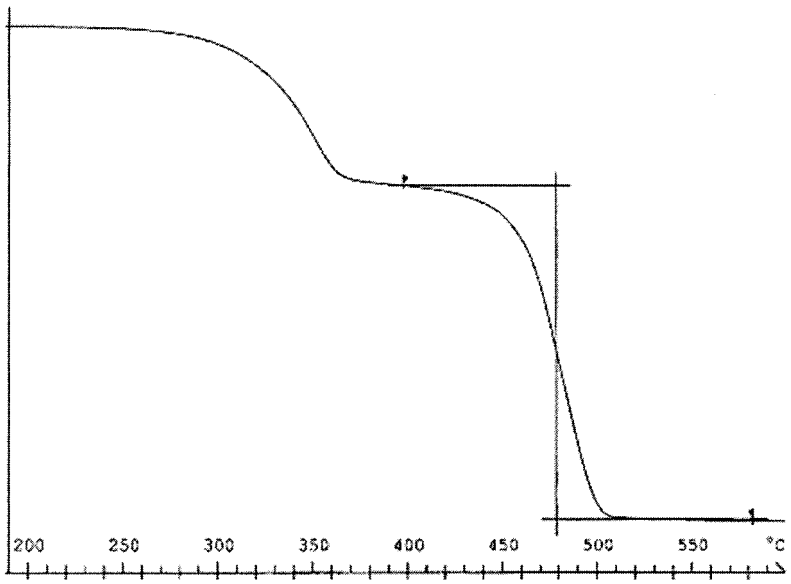

Figure 2 Typical TGA curve of a composite.

cated between the fiber content and the increasing MAPP content of the composites. The influence of the sample location in the tensile specimen on the fiber content was studied with composite C1. The samples for TGA measurements were taken from composite C1 at the locations shown in Figure 3. The TGA results (given next to the sample locations in Fig. 3) indicate that the fiber content in the composite increases with the distance from the nozzle of the injection-molding machine. The difference in content is probably due to the different rheological properties of the fiber and PP.

Effect of the coupling agent on the mechanical properties of the composites

The mechanical properties of pure PP and composites A–C were evaluated with tensile tests, and the results are given in Table IV. The results for the composites indicate that the tensile strength, yield strength, fracture energy, elongation at fracture, and fracture strength improve with the MAPP content. These improvements are due to the better interfacial adhesion, which promotes stress transfer from the matrix to the fiber. If MAPP is not used in the composite, the tip of the fracture, when it encounters the fiber, advance along the fiber–matrix interphase.

A comparison of the mechanical properties of the composites, with and without MAPP, with the properties of pure PP shows that the tensile strength, yield strength, and fracture strength are increased in the composites. The fracture energy is determined from the area under the stress–strain curve up to the point of fracture. Although the tensile strength of PP is less than that of the composites, the elongation at fracture and, therefore, the fracture energy are much higher for PP than for the composites. More work is required to break the pure matrix than to break the composite. The mechanical properties of the composites, especially the tensile strength, are greatly improved in comparison with previous PP/MAPP/wood-fiber composite studies.[14,15]

Morphology and dispersion of the composites

The morphology of the fractured composite surfaces was investigated with SEM. The fracture surface of the composite containing 6% MAPP (C2) was compared

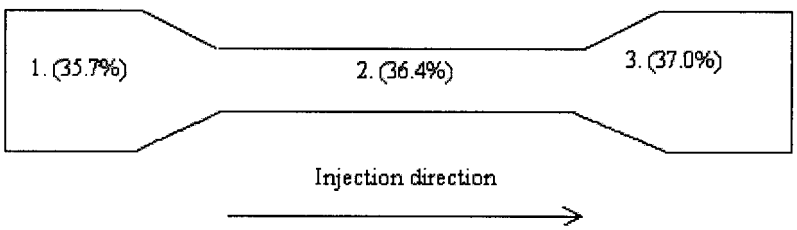

Figure 3 Tensile specimen C1, with the TGA sample locations and fiber contents given.

TABLE IV
Results of the Tensile Tests

Series	Statistic	Yield strength (MPa)	Tensile modulus (GPa)	Fracture strength (MPa)	Fracture energy (J/mm^2)	Tensile strength (MPa)	Elongation at fracture (%)
PP	$n = 7$						
	Average	15.04	1.93	16.18	1.96	35.39	261.62
	SD	1.43	0.17	5.56	0.86	0.64	139.91
A	$n = 5$						
	Average	23.35	3.69	36.79	0.06	37.62	5.58
	SD	0.96	0.19	0.21	0.01	0.30	0.63
B	$n = 5$						
	Average	35.16	3.72	67.37	0.127	68.41	6.92
	SD	0.93	0.10	1.84	0.004	0.71	0.12
C	$n = 6$						
	Average	33.83	3.68	68.81	0.14	69.12	7.43
	SD	2.19	0.30	1.76	0.01	1.27	0.23

SD = standard deviation.

with that of the composite that had no MAPP (A2) in an attempt to clarify the reinforcement mechanism in composites containing MAPP. Figures 4 and 5 show SEM pictures of the fiber–matrix interphases. The interphase without MAPP (Fig. 4) is clearly cracked because of the lack of interfacial adhesion. Comparing the fiber ends, we can see that the fiber in the MAPP-containing composite (Fig. 5) is fractured, whereas the fiber in the composite without MAPP clearly is not.

In the composites in which a coupling agent is not used (Fig. 4), the fracture surface is covered with fibers that have been pulled out from the matrix. Fiber pull-out is a well known result of interfacial adhesion.[14,16–18] Some holes can be seen in the MAPP-treated composite as well, but fibers that were pulled out are hard to detect. The fiber and the matrix possess different Poisson ratios, and the resulting Poisson effect is known to have a negative influence on fiber–matrix adhesion in composites.[19,20] The Poisson effect may partly explain the cracked interface seen in Figure 4. MAPP binds the two phases together, preventing the Poisson effect, and the fiber–matrix interface does not crack so readily (Fig. 5).

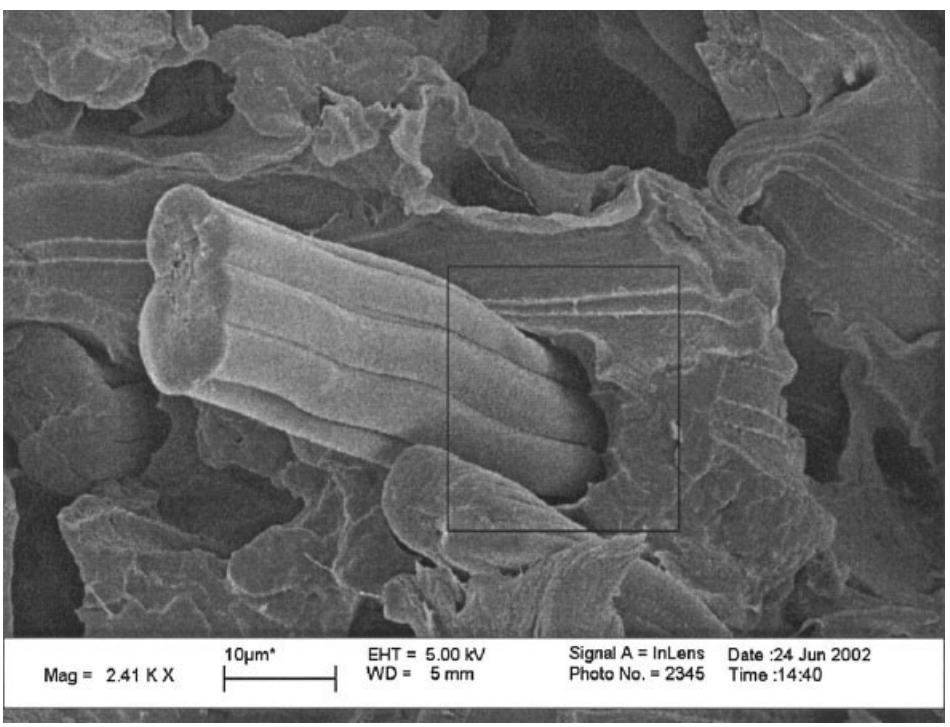

Figure 4 SEM picture of the fiber–matrix interface of the fracture surface of tensile specimen A2.

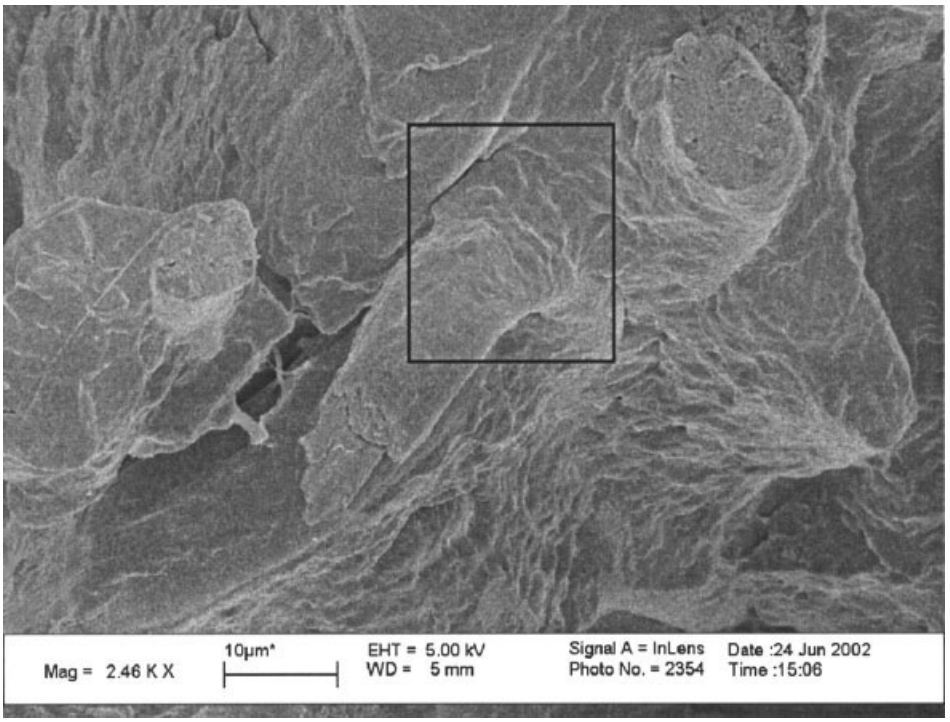

Figure 5 SEM picture of the fiber–matrix interface of the fracture surface of tensile specimen C2.

Unlike inorganic fibers, viscose and natural cellulose fibers are flexible. This can be seen in the area framed with a rectangle in Figure 6, in which a fiber end is bent 180°. In Figure 4, we can see how the surface of a viscose fiber differs from that of pulped or natural fibers.[15,21] A viscose fiber can be described as a fiber bundle consisting of thin, round fibers, which create grooves on the surface of the bundle. One effect

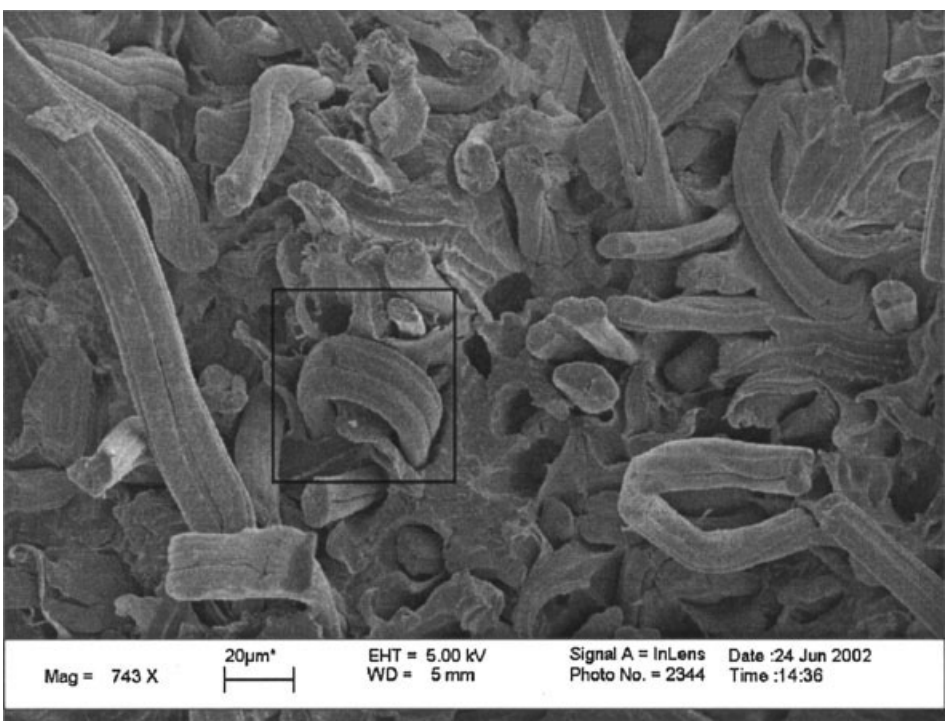

Figure 6 Fracture surface of the tensile specimen A2.

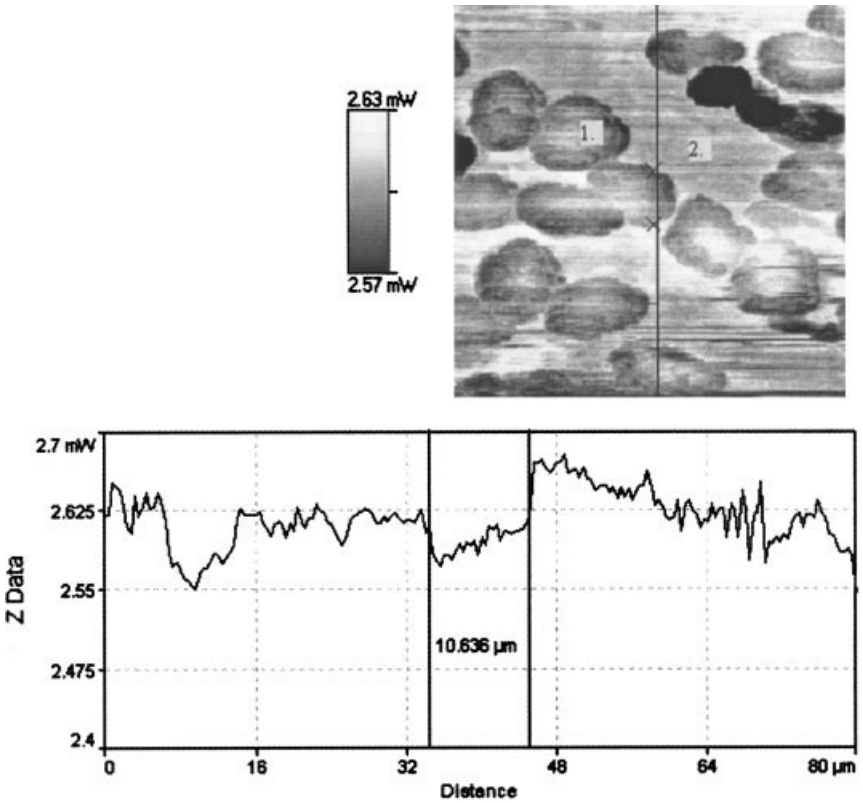

Figure 7 Micro-TA conductivity image of a sample surface of tensile specimen B2. The numbers indicate the locations of the local thermal analyses. The curve presents a conductivity profile taken at the line (top to bottom on the line is presented as left to right on the profile).

of the grooves is to produce a large surface area, which may have a positive effect on the adhesion when MAPP is added as a coupling agent. Figure 5 shows the grooves on the fiber surface covered with a material, most likely MAPP, that is chemically bound to the surface of the fiber.

A new scanning thermal microscopy method, micro-TA, was used to investigate the clustering of the fibers on the microtome-cut surfaces of the tensile specimens. Micro-TA allows the measurement of the thermal conductivity and the recording of thermal diffusivity images from the surface. In addition, local thermal analysis can be carried out on different parts of the surface.[22,23]

Conductivity and topographical images were recorded from the cross sections of the composites. Figure 7 show the conductivity image obtained from the cross section of sample B2. The areas of the fibers (thermal conductivity = 0.054–0.07 W m^{-1} K^{-1})[24] show up darker than the areas of the matrix (thermal conductivity = 0.12 W m^{-1} K^{-1}).[25] Micro-TA is able to differentiate the fibers from the matrix on the basis of the conductivity difference, although the rough topography and only a small conductivity difference between the fiber and the matrix may make it difficult to obtain good-quality images (i.e., the contrast between the phases is low). Wei et al.[26] reported similar difficulties with PP–glass composites.

The authenticity of the conductivity image can be verified by the recording of heating curves at the location of the fiber and the matrix. Figure 7 shows the locations of the local thermal analyses, and Figure 8 illustrates the measured heating profiles. The melting at location 2 was observed as a downward movement of the tip. The measured melting point was about 160°C and indicated the presence of the PP matrix. Melting did not occur at the location of fiber (location 1), as can be seen from the continually rising curve in Figure 8.

On the basis of the AFM results, MAPP had no notable effect on the clustering of the fibers. According to the measured images, the dispersion was adequate in all composites. The diameters of the fibers were obtained with a line measure. Four images were examined for each MAPP content (samples A1, B2, and C2), and six values were taken from each image. The diameter of the fibers varied from 10 to 20 μm, but the average diameter was about 15 μm, regardless of the MAPP content of the composite. The same values were obtained with SEM. The diameter of the viscose fibers is small compared

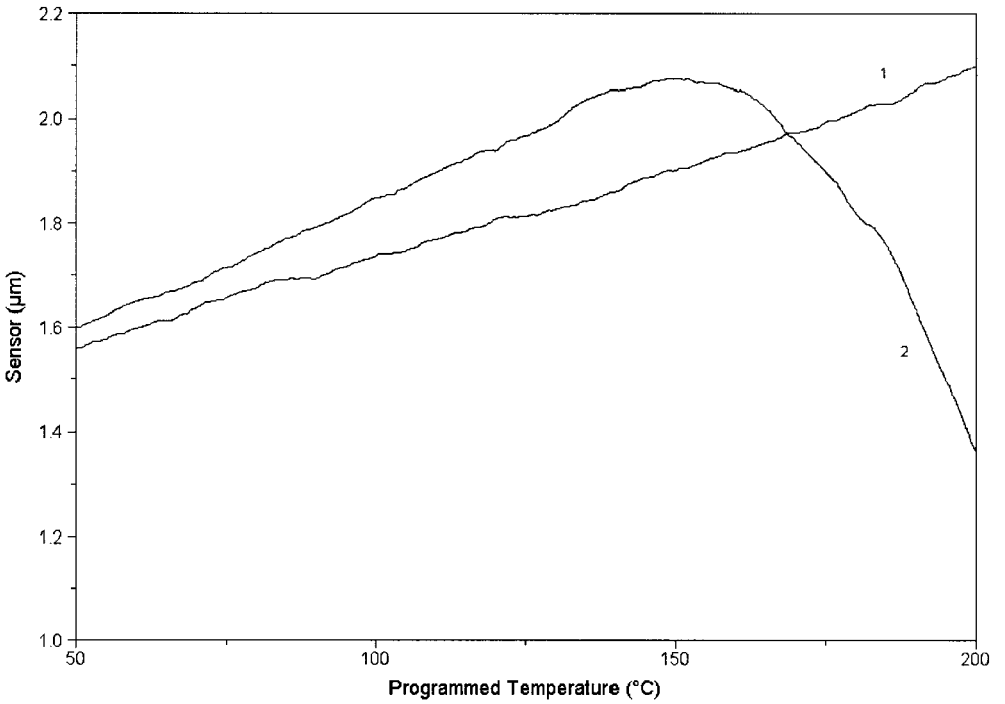

Figure 8 Sensor height position versus the temperature at locations 1 and 2 of sample B2 (see Fig. 7).

with that of natural fibers.[21] The smaller diameter allows a shorter critical length of the fibers in the composites, thereby improving the mechanical reinforcement of the continuous fiber composites. The following formula describes the dependence of the critical length (l_c) in continuous fiber composites on the diameter of the fiber:[27]

$$l_c = \frac{\sigma^* d}{2\tau_c}$$

The variable σ^* is the ultimate tensile strength of the fiber, and τ_c is the fiber–matrix bond strength. The use of MAPP also reduces the critical fiber length by increasing the strength of the fiber–matrix bond.[14]

CONCLUSIONS

This work investigated the effects of a coupling agent, MAPP, on the composition and morphology of injection-molded viscose-fiber PP composites. The following conclusions were drawn:

- TGA offered a convenient method for measuring the cellulose-fiber contents of PP composites.
- The mechanical properties improved when MAPP was added as a coupling agent. SEM pictures showed that the poor tensile properties of the composites that did not contain MAPP were the result of fiber pullout and fiber–matrix fracture.
- An examination of the fiber clustering of the composites by micro-TA showed that composites containing different levels of MAPP were not very different. A low conductivity difference between the fiber and the matrix and the rough topography complicated the recording of conductivity images. Local thermal analyses were able to detect the fiber and matrix in the composite more effectively.

The Crompton Corp. is thanked for the information and material assistance that it provided.

References

1. Bledzki, A. K.; Gassan, J. Prog Polym Sci 1999, 24, 221.
2. Mohanthy, A. K.; Mishra, M.; Hinrichsen, G. Macromol Mater Eng 2000, 276, 1.
3. Blendzki, A. K.; Reihmane, S.; Gassan, J. Polym Plast Technol Eng 1998, 37, 451.
4. Lu, J. Z.; Wu, Q.; Mcnabb, H. S., Jr. Wood Fiber Sci 2000, 32, 88.
5. Mai, K.; Mäder, E.; Mühle, M. Compos A 1998, 29, 1111.
6. Munz, M.; Sturm, H.; Schulz, E.; Hinrichsen, G. Compos A 1998, 29, 1251.
7. Marieta, C.; Schulz, E.; Mondragon, I. Compos Sci Technol 2002, 62, 299.
8. Argyropoulos, D. S. Advances in Lignocellulosic Characterization; Tappi: Atlanta, TX, 1999; p 337.
9. Mahlberg, R.; Niemi, H. E.-M.; Denes, F. S.; Rowell, R. M. Langmuir 1999, 15, 2985.

10. Vovelle, C.; Mellottee, H.; Delbourgo, R. Symp Combust/Combust Inst 1982, 19, 797.
11. Price, D.; Horrocks, A. R.; Akalin, M.; Faroq, A. A. J Anal Appl Pyrolysis 1997, 40, 511.
12. Wielage, B.; Lampke, T.; Marx, G.; Nestler, K.; Starke, D. Thermochim Acta 1999, 337, 169.
13. Yee, R. Y.; Stephens, T. S. Thermochim Acta 1996, 272, 191.
14. Felix, J. M.; Gatenholm, P. J Appl Polym Sci 1991, 42, 609.
15. Quek, M. Y.; Yue, C. Y. Mater Sci Eng A 1994, 189, 105.
16. Neus Angles, M.; Salvado, J.; Dufresne, A. J Appl Polym Sci 1999, 74, 1962.
17. Stark, N. M. Forest Prod J 1999, 49, 39.
18. Glasser, W. G.; Taib, R.; Jain, R. K.; Kander, R. J Appl Polym Sci 1999, 73, 1329.
19. Kalantar, J.; Drzal, L. T. J Mater Sci 1990, 25, 4194.
20. Kazayawako, M.; Balatinecz, J. J.; Woodhams, R. T.; Law, S. J Reinforced Plast Compos 1997, 16, 1383.
21. Eichhorn, S. J.; Baillie, C. A.; Zafeiropoulos, N.; Mwaikambo, L. Y.; Ansell, M. P.; Dufresne, A.; Entwistle, K. M.; Herrera-Franco, P. J.; Escamilla, G. C.; Groom, L.; Hughes, M.; Hill, C.; Rials, T. G.; Wild, P. M. J Mater Sci 2001, 36, 2107.
22. Song, M.; Hourston, D. J.; Grandy, D. B.; Reading, M. J Appl Polym Sci 2001, 81, 2136.
23. Tsukruk, V. V.; Gorbunov, V. V.; Fuchigami, N. Thermochim Acta 2002, 7043, 1.
24. Brandrup, J.; Immergut, E. H.; Grulke, E. A. Polymer Handbook, 4th ed.; Wiley: New York, 1999; Vol. 5, p 152.
25. Callister, W. D., Jr. Materials Science and Engineering: An Introduction, 5th ed.; Wiley: New York, 2000; p 662.
26. Wei, X.; Sisk, B.; Gao, Z.; Pan, W.-P. Proc NATAS Annu Conf Therm Anal Appl 2000, 28, 45.
27. Callister, W. D., Jr. Materials Science and Engineering: An Introduction, 5th ed.; Wiley: New York, 2000; p 528.